# Temperature-Dependent Transformation Thermotics: From Switchable Thermal Cloaks to Macroscopic Thermal Diodes

Ying Li,[2] Xiangying Shen,[1] Zuhui Wu,[1] Junying Huang,[1] Yixuan Chen,[1] Yushan Ni,[2] and Jiping Huang[1,*]
[1]Department of Physics, State Key Laboratory of Surface Physics, Key Laboratory of Micro and Nano Photonic Structures (Ministry of Education), and Collaborative Innovation Center of Advanced Microstructures, Fudan University, Shanghai 200433, China
[2]Department of Mechanics and Engineering Science, Fudan University, Shanghai 200433, China
(Received 22 May 2015; published 5 November 2015)

The macroscopic control of ubiquitous heat flow remains poorly explored due to the lack of a fundamental theoretical method. Here, by establishing temperature-dependent transformation thermotics for treating materials whose conductivity depends on temperature, we show analytical and simulation evidence for switchable thermal cloaking and a macroscopic thermal diode based on the cloaking. The latter allows heat flow in one direction but prohibits the flow in the opposite direction, which is also confirmed by our experiments. Our results suggest that the temperature-dependent transformation thermotics could be a fundamental theoretical method for achieving macroscopic heat rectification, and it could provide guidance both for the macroscopic control of heat flow and for the design of the counterparts of switchable thermal cloaks or macroscopic thermal diodes in other fields like seismology, acoustics, electromagnetics, and matter waves.

DOI: 10.1103/PhysRevLett.115.195503 PACS numbers: 81.05.Xj, 44.90.+c, 74.25.fc

Heat flow is a ubiquitous phenomenon in nature, and hence how to control the flow of heat at will is of particular importance for human life. Fortunately, the past years have witnessed the possibility of manipulating phononic [1–7] or electronic [8–11] heat conduction at the nanoscale, which provides a promising method for making use of heat flux. To date, significant progress has been made, such as computation [3], information storage [4], and caloritronics [8,9]. On the contrary, steering heat conduction at the macroscale is still far from satisfactory [12], which prohibits macroscopic thermal rectification for diverse thermal management problems, e.g., efficient refrigerators, solar cells, and energy-saving buildings [13–15]. A reason behind the situation is the lack of a fundamental theoretical method.

In 2008, Fan *et al.*. [16] adopted a coordinate transformation approach to propose a class of thermal metamaterial where heat is caused to flow around an "invisible" region at steady state, thus called thermal cloaking. The cloaking originates from the fact that the thermal conduction equation remains form invariant under coordinate transformation. So far, the theoretical proposal of steady-state thermal cloaking [16] and its extensions (say, bifunctional cloaking of heat and electricity [17] or nonsteady-state thermal cloaking [18]) have been experimentally verified and developed [19–23]. The theoretical treatment based on coordinate transformation [16–18,24–28], which is called transformation thermotics (or transformation thermodynamics), has the potential to become a fundamental theoretical method for macroscopically manipulating heat flow at will.

However, in order to realize desired macroscopic thermal rectification, say, switchable thermal cloaking and macroscopic thermal diodes, the existing transformation thermotics [16–18] is not enough since it only holds for materials whose conductivity is independent of temperature (thus called linear materials). For instance, the desired thermal diode should conduct heat in one direction but insulate the heat in the opposite direction. This is a kind of asymmetric behavior of the heat current. For this purpose, nonlinear materials (whose conductivity relies on temperature) must be adopted. Actually, it has long been known that for many materials, their thermal conductivities ($\kappa$) vary with temperature ($T$). (1) $\kappa$ increases as $T$ increases. Say, for noncrystalline solids, a series of experiments on glass [29] showed that at low temperature the thermal conductivity is proportional to $T^{1.6} \sim T^{1.8}$. (2) $\kappa$ increases as $T$ decreases. For example, measurements on single crystals of silicon and germanium from 3 K to their melting point [30] showed that their thermal conductivity decreases faster than $1/T$.

*Temperature-dependent transformation thermotics.*— Now, we are in a position to establish a theory of transformation thermotics for treating nonlinear materials, thus called temperature-dependent transformation thermotics. The details of the theory are given in Part I of Ref. [31], which yields the key formula, Eq. (S8), namely, $\tilde{\kappa}(T) = \tilde{J}(T)\kappa_0\tilde{J}^{\mathrm{t}}(T)/\det[\tilde{J}(T)]$, where $\tilde{\kappa}(T)$ is the $T$-dependent thermal conductivity of the device, $\kappa_0$ the $T$-independent thermal conductivity of the background, $\tilde{J}(T)$ the $T$-dependent Jacobian matrix, $\tilde{J}^{\mathrm{t}}(T)$ the transpose of $\tilde{J}(T)$, and $\det[\tilde{J}(T)]$ the determinant of $\tilde{J}(T)$. Equation (S8) denotes that instead of constructing materials for a background whose thermal conductivity is $T$ dependent, we may apply a $T$-involved transformation $\tilde{J}(T)$ to the original

 

thermal conduction equation. This process allows us to design switchable thermal cloaks and then macroscopic thermal diodes. The former serve as an extension of the extensively investigated cloaks without switches [16–23,32]; the latter are actually a useful application of the former in this work. We proceed as follows.

*Switchable thermal cloaks.*—Design: A traditional thermal cloak can protect a central region from an external heat flux and permits the region to remain a constant temperature without disturbing the temperature distribution outside the cloak (Fig. 1). To achieve this cloaking effect, a simple radial stretch transformation of polar coordinates may be performed. As schematically shown in Fig. 1, the circular region with radius $R_2$ is compressed to the annulus region with radius in between $R_1$ and $R_2$, and the geometrical transformation can be written as

$$r' = r\frac{R_2 - R_1}{R_2} + R_1, \tag{1}$$

where $r \in [0, R_2]$ and $r' \in [R_1, R_2]$. Here, $r'$ is the radial coordinate in physical space.

In order to realize different responses to heat flow on the two sides of a thermal diode, we need two types of thermal cloaks: one functions at high temperature (hereafter indicated as type-$A$ cloaks), the other works at low temperature (type-$B$ cloaks). Unlike some previously proposed switchable electromagnetic cloaks [33–35], the switching effect should be triggered automatically by temperature changes. For this purpose, an idea is to modify Eq. (1) as

$$r' = r\frac{R_2 - \tilde{R}_1(T)}{R_2} + \tilde{R}_1(T), \tag{2}$$

where $\tilde{R}_1(T) = R_1[1 - (1 + e^{\beta(T-T_c)})^{-1}]$ for type-$A$ cloaks and $\tilde{R}_1(T) = R_1/(1 + e^{\beta(T-T_c)})$ for type-$B$ cloaks. Here, $T_c$ is a critical temperature around which the cloak is switched on or off, and $\beta$ is a scaling coefficient which is set to be 2.5 $K^{-1}$ in this work.

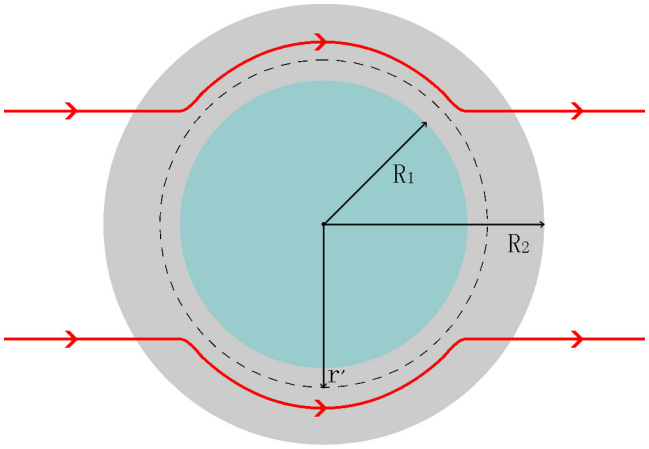


FIG. 1 (color online). Schematic graph depicting a thermal cloak between radius $R_1$ and $R_2$. The red lines with arrows denote the flow of heat: the cloak does not disturb the heat flow at a region with a radius larger than $R_2$; the heat flux cannot enter a central region with a radius smaller than $R_1$.

So far, for obtaining thermal cloaks with switching phenomena, we need to combine Eqs. (2) and (S8). As a result, for the area with radius $r' \in [R_1, R_2]$ in Fig. 1, we achieve the thermal conductivities in polar coordinates, $\mathrm{diag}[\tilde{\kappa}_r(T), \tilde{\kappa}_\theta(T)]$, as

$$\tilde{\kappa}_r(T) = \kappa_0 \frac{r' - \tilde{R}_1(T)}{r'}, \qquad \tilde{\kappa}_\theta(T) = \kappa_0 \frac{r'}{r' - \tilde{R}_1(T)}. \tag{3}$$

Here, $\kappa_0$ represents the $T$-independent thermal conductivity of the background.

Finite-element simulations: Then we perform finite-element simulations based on the commercial software COMSOL Multiphysics. A thermal cloak with $R_1 = 1$ cm and $R_2 = 2$ cm is set in a box with size 8 cm × 7 cm, as shown in Fig. 2. Heat diffuses from the left boundary with high temperature $T_H$ to the right boundary with low temperature $T_L$. Meanwhile, the upper and lower boundaries of the simulation box are thermally isolated.

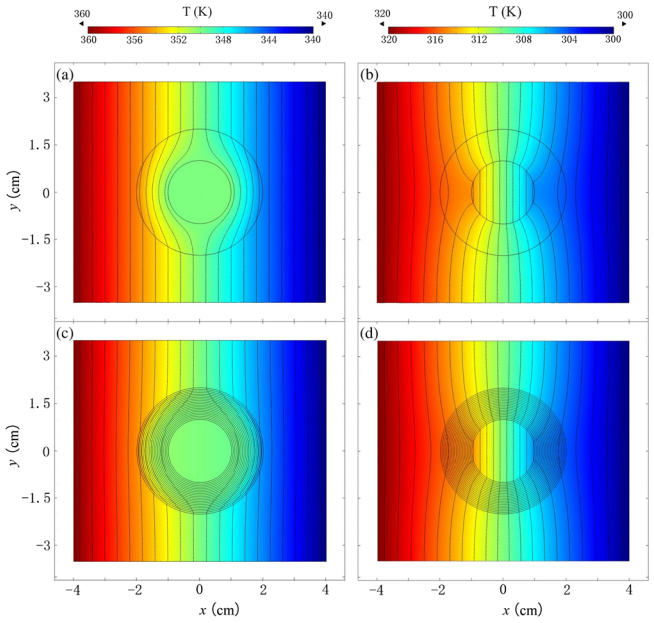


FIG. 2 (color online). Switchable thermal cloaks obtained by two-dimensional finite-element simulations: (a),(c) switch on for the temperature above 340 K and (b),(d) switch off for the temperature below 320 K. The color surface denotes the distribution of temperature, where isothermal lines are indicated; heat diffuses from left to right; the upper and lower boundaries are the thermal insulation. (a) and (b) show the results of thermal conductivities calculated according to Eq. (3); (c) and (d) show the results of ten alternating layers of two sublayers, with $\kappa_1(T)$ and $\kappa_2(T)$ given by Eq. (4) (EMT). In (a)–(d), an object with thermal conductivity 0.01 W/mK is set in the central region with radius $R_1$. Parameters: $\kappa_0 = 1$ W/mK, $\kappa_a = 0.1$ W/mK, $\kappa_b = 10$ W/mK, $R_1 = 1$ cm, $R_2 = 2$ cm, and $T_c = 330$ K.

The simulation results of a type-$A$ cloak are shown in Figs. 2(a) and 2(b). In Fig. 2(a), at high temperature ($T = 340$–$360$ K), we observe that the cloak is functioning and thermally hiding the object located at the central region with radius $R_1$. However, when the environment is changed to low temperature ($T = 300$–$320$ K), the cloak is turned off. That is, the temperature distribution outside the object is distorted, just as the cloak (located between $R_1$ and $R_2$) is absent. Owing to the antisymmetry between type-$A$ and type-$B$ cloaks, the type-$B$ cloaks exhibit behavior similar to Figs. 2(a) and 2(b), but switching on (or off) at low (or high) temperature.

Theoretical realization based on the effective medium theory: The materials designed according to Eq. (3) are anisotropic and inhomogeneous, which is difficult to realize in experiments. In fact, for constructing such materials, we can simply utilize alternating layers of two homogeneous isotropic sublayers with thicknesses $d_1$ and $d_2$ and conductivities $\kappa_a$ and $\kappa_b$. For simplification, in this Letter, we set $d_1 = d_2$. According to the theoretical analysis and effective medium theory (EMT) [17–19,32,36], the conductivities of two sublayers should satisfy $\kappa_a\kappa_b \approx \kappa_0^2$ for a traditional cloak. In order to endue conventional cloaks with the switching effect, some mathematical operations must be carried out on $\kappa_a$ and $\kappa_b$ in a way that is analogous to what we did on $\tilde{R}_1(T)$. Therefore, we obtain $\kappa_1(T)$ and $\kappa_2(T)$ as the new temperature-dependent thermal conductivities of the sublayers,

$$\kappa_1(T) = \kappa_a + \frac{\kappa_0 - \kappa_a}{1 + e^{\beta(T-T_C)}}, \qquad \kappa_2(T) = \kappa_b - \frac{\kappa_b - \kappa_0}{1 + e^{\beta(T-T_C)}}. \tag{4}$$

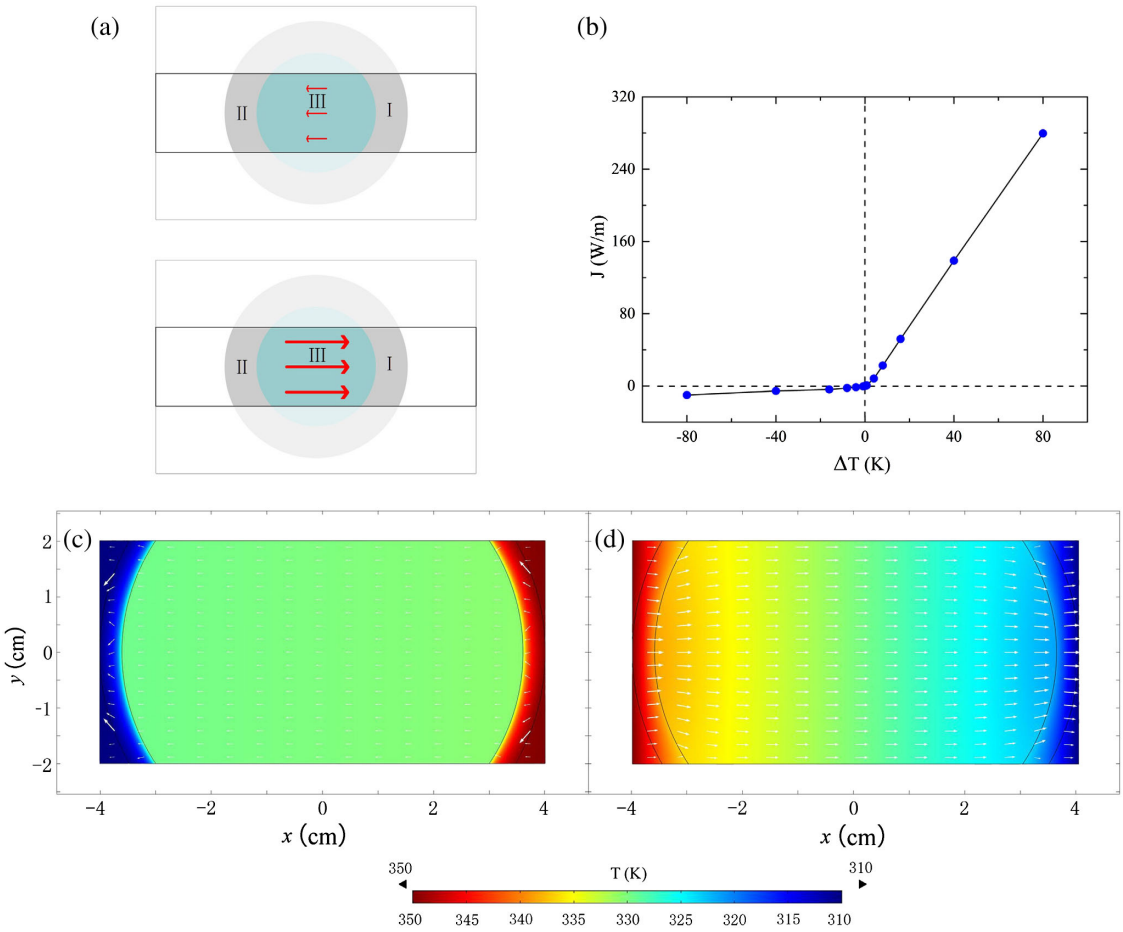


FIG. 3 (color online). (a) Sketch of a thermal diode, which is the rectangular area enclosed by the solid black lines. The blurred area outside is a reference and actually does not exist in the design. I, II, and III represent three regions, respectively. Here, the arrows indicate the direction of heat flow; the length of the arrows represents the amount of heat flux: the heat flux transferred from right to left (upper panel, the insulating case) is much smaller than that from left to right (lower panel, the conducting case). (b) Heat current $J$ versus temperature bias $\Delta T$. (c),(d) Thermal diode obtained by two-dimensional finite-element simulations: (c) the insulating case and (d) the conducting case. The color surface denotes the distribution of temperature; the white arrows represent the direction of heat flow; the length of the white arrows indicates the amount of heat flux; the upper and lower boundaries are the thermal insulation. Thermal conductivities are calculated according to Eq. (3); an object with thermal conductivity 10 W/mK is set in the central region with radius $R_1$. Parameters: $\kappa_0 = 1$ W/mK, $R_1 = 3.6$ cm, $R_2 = 4$ cm, and $T_c = 330$ K.

The two expressions yield $\kappa_1(T) \to \kappa_a$ and $\kappa_2(T) \to \kappa_b$ when $T \gg T_C$; $\kappa_1(T) \to \kappa_0$ and $\kappa_2(T) \to \kappa_0$ as $T \ll T_C$. [The detailed dependence of $\kappa_1(T)$ and $\kappa_2(T)$ on temperature is displayed in Fig. S3 of Part III of Ref. [31].] That is, the cloaking effect is switched on (or off) for high (or low) temperature environment $T \gg T_C$ (or $T \ll T_C$). Equation (4) offers a convenient tool for helping us to experimentally realize our theoretical design of Eq. (3). Next, we plot Figs. 2(c) and 2(d), which shows the simulation results of ten alternating layers for constructing type-$A$ cloaks. Evidently, Figs. 2(c) and 2(d) display a switching phenomenon similar to Figs. 2(a) and 2(b). The procedure holds the same for achieving type-$B$ cloaks.

*Macroscopic thermal diode.*—Design: The above thermal cloaking may help us to design a kind of macroscopic thermal diode. As shown in Fig. 3(a), the diode device contains regions I, II, and III: region I (II) is a segment of the type-$A$ (type-$B$) cloak, and region III is a thermal conductor. Compared with a full system, the cloaking effect still exists in our diode, but it is not perfect. There will be a small amount of heat flux conducting through the central region for the insulating case. However, the truncation of a whole cloak is necessary to separate the type-$A$ part and the type-$B$ part. The antisymmetry of type-$A$ and type-$B$ cloaks is expected to cause different behaviors of heat conducting from the two opposite directions. The transformation plays an important role in introducing anisotropic effect to the structure, which guides the heat flux to the boundaries to enhance the thermal insulating effect.

Finite-element simulations: Then we perform finite-element simulations. Figures 3(c) and 3(d) show the simulation results of the device, which helps us to insulate heat from right to left but conduct the heat from left to right. That is, the behavior of the diode can indeed be achieved due to the antisymmetry of type-$A$ and type-$B$ cloaks (namely, region I and region II). Moreover, for different temperature biases (obtained by subtracting the temperature at the right boundary from that at the left boundary), $\Delta T$, we also calculate the total heat current $J$ by integrating the $x$ component of heat flux across the line $x = 0$; see Fig. 3(b). The device displays a significant rectifying effect, which has a maximum rectification ratio of 30 for the current parameter set.

Experimental realization based on the effective medium theory: In order to realize such a macroscopic thermal diode, we can also adopt the EMT. As discussed above, the switchable thermal cloak can be constructed with alternating layers. The thermal conductivities of the sublayers are required to be sensitive to the temperature change around the critical point. This kind of behavior can be found in the phase transitions of certain materials [37–39]. However, inspired by the spirit of metamaterials (yielding novel functions by assembling conventional materials into specific structures), we manage to realize the macroscopic thermal diode with materials of constant conductivities. Our method is that, instead of directly resorting to the transitions of materials' physical properties, we use the structural transition to trigger the switching effect. According to the demands of our design, the geometrical configuration of the device should change rapidly as temperature varies. Fortunately, we found that the shape-memory alloy (SMA) [40] may be able to help. As shown in the schematic diagrams of our design [see Figs. 4(a) and 4(b); more details of our experiment can be found in Part II of Ref. [31]], the sublayers of the cloak segments are coppers and expanded polystyrene (EPS). Around the critical temperature, the deformations of the SMA slices drive the copper slices to connect or disconnect the copper layers. The connection and disconnection can be equivalently regarded as transitions of the local thermal conductivities. Thus, a temperature-dependent thermal metamaterial is realized with materials of constant thermal conductivities (a whole switchable thermal cloak can also be built with the same method). The experimental results are shown in Figs. 4(c) and 4(d). Figure 4(c) displays the temperature distribution within the central region, which is almost constant. That is, in this case, heat almost cannot flow through this central region. Thus, Fig. 4(c) corresponds to the insulating case of the diode. In contrast, Fig. 4(d) represents the conducting case of the diode. This is because Fig. 4(d) shows a significant temperature

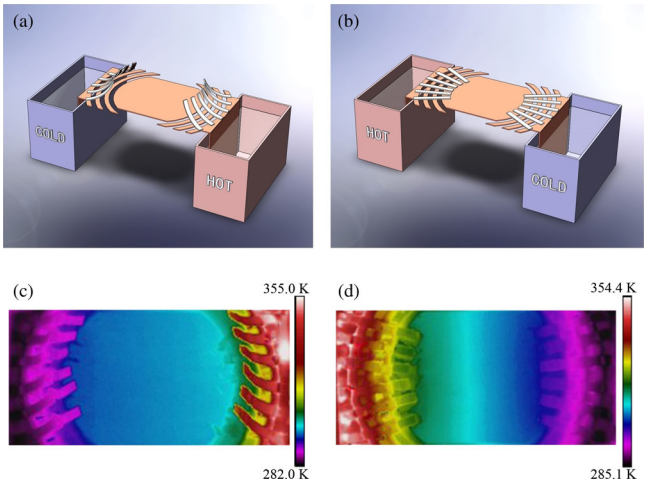


FIG. 4 (color online). (a),(b) Scheme of experimental demonstration of the macroscopic thermal diode: (a) insulating case and (b) conducting case. Both the copper-made concentric layered structure and the central copper plate (both displayed in orange) are placed on an EPS plate which, for the sake of clarity, is not shown. The left and right sides of the diode are stuck in water to promote constant temperature boundary conditions. (a) When cold water is filled in the left container (light blue) and hot water in the right container (pale red), the bimetallic strips of SMA and copper (white) warp up and the device blocks heat from right to left. (b) When the two containers swap their locations, the bimetallic strips (white) flatten and the device conducts heat from left to right. (c),(d) Experimentally measured temperature distribution of the device: (c) insulating case and (d) conducting case.

gradient within the central region. Also, the temperature distribution appears to be horizontal. As a result, we can conclude that an evident heat flow starts to appear within the central region of Fig. 4(d).

*Conclusions.*—We have established a theory of temperature-dependent transformation thermotics for dealing with thermal materials whose conductivity is temperature dependent. The theory serves as a fundamental theoretical method for designing switchable thermal cloaking. We have also shown that the switchable thermal cloaks can be employed for achieving a macroscopic thermal diode, which has also been experimentally realized by assembling homogeneous and isotropic materials according to the design based on the EMT. The diode has plenty of potential applications related to heat preservation, heat dissipation, and even heat illusion [41,42] in many areas, like efficient refrigerators, solar cells, energy-saving buildings, and military camouflage. Thus, by using temperature-dependent transformation thermotics to tailor nonlinear effects appropriately, it becomes possible to achieve desired thermal metamaterials with diverse capacities for macroscopic thermal rectification. On the same footing, our consideration (for cloaks and diodes) adopted in this work can be extended to obtain the counterparts of both switchable thermal cloaks and macroscopic thermal diodes in other fields like seismology, acoustics, electromagnetics, and matter waves.

We acknowledge the financial support of the National Natural Science Foundation of China under Grants No. 11222544 and No. 11572090 (Y. L. and Y. N.), of the Fok Ying Tung Education Foundation under Grant No. 131008, of the Program for New Century Excellent Talents in University (Grant No. NCET-12-0121), and of the CNKBRSF under Grant No. 2011CB922004.

Y. L. and X. S. contributed equally to this work.

*jphuang@fudan.edu.cn.

[1] B. Li, L. Wang, and G. Casati, Phys. Rev. Lett. **93**, 184301 (2004).
[2] C. W. Chang, D. Okawa, A. Majumdar, and A. Zettl, Science **314**, 1121 (2006).
[3] L. Wang and B. Li, Phys. Rev. Lett. **99**, 177208 (2007).
[4] L. Wang and B. Li, Phys. Rev. Lett. **101**, 267203 (2008).
[5] N. Li, J. Ren, L. Wang, G. Zhang, P. Hanggi, and B. Li, Rev. Mod. Phys. **84**, 1045 (2012).
[6] M. Maldovan, Nature (London) **503**, 209 (2013).
[7] Z. Chen, C. Wong, S. Lubner, S. Yee, J. Miller, W. Jang, C. Hardin, A. Fong, J. E. Garay, and C. Dames, Nat. Commun. **5**, 5446 (2014).
[8] F. Giazotto and M. J. Martínez-Pérez, Nature (London) **492**, 401 (2012).
[9] M. J. Martínez-Pérez and F. Giazotto, Nat. Commun. **5**, 3579 (2014).
[10] A. Fornieri, M. J. Martínez-Pérez, and F. Giazotto, Appl. Phys. Lett. **104**, 183108 (2014).
[11] M. J. Martínez-Pérez, A. Fornieri, and F. Giazotto, Nat. Nanotechnol. **10**, 303 (2015).
[12] Y. Wang, A. Vallabhaneni, J. Hu, B. Qiu, Y. P. Chen, and X. Ruan, Nano Lett. **14**, 592 (2014).
[13] W. Kobayashi, Y. Teraoka, and I. Terasaki, Appl. Phys. Lett. **95**, 171905 (2009).
[14] D. Go and M. Sen, J. Heat Transfer **132**, 124502 (2010).
[15] W. Kobayashi, D. Sawaki, T. Omura, T. Katsufuji, Y. Moritomo, and I. Terasaki, Appl. Phys. Express **5**, 027302 (2012).
[16] C. Z. Fan, Y. Gao, and J. P. Huang, Appl. Phys. Lett. **92**, 251907 (2008).
[17] J. Y. Li, Y. Gao, and J. P. Huang, J. Appl. Phys. **108**, 074504 (2010).
[18] S. Guenneau, C. Amra, and D. Veynante, Opt. Express **20**, 8207 (2012).
[19] S. Narayana and Y. Sato, Phys. Rev. Lett. **108**, 214303 (2012).
[20] R. Schittny, M. Kadic, S. Guenneau, and M. Wegener, Phys. Rev. Lett. **110**, 195901 (2013).
[21] H. Xu, X. Shi, F. Gao, H. Sun, and B. Zhang, Phys. Rev. Lett. **112**, 054301 (2014).
[22] T. Han, X. Bai, D. Gao, J. T. L. Thong, B. Li, and C.-W. Qiu, Phys. Rev. Lett. **112**, 054302 (2014).
[23] Y. Ma, Y. Liu, M. Raza, Y. Wang, and S. He, Phys. Rev. Lett. **113**, 205501 (2014).
[24] U. Leonhardt, Science **312**, 1777 (2006).
[25] J. B. Pendry, D. Schurig, and D. R. Smith, Science **312**, 1780 (2006).
[26] H. Chen, C. T. Chan, and P. Sheng, Nat. Mater. **9**, 387 (2010).
[27] N. Landy and D. R. Smith, Nat. Mater. **12**, 25 (2013).
[28] M. Kadic, T. Bückmann, R. Schittny, and M. Wegener, Rep. Prog. Phys. **76**, 126501 (2013).
[29] R. C. Zeller and R. O. Pohl, Phys. Rev. B **4**, 2029 (1971).
[30] C. J. Glassbrenner and G. A. Slack, Phys. Rev. **134**, A1058 (1964).
[31] See Supplemental Material at http://link.aps.org/supplemental/10.1103/PhysRevLett.115.195503 for temperature-dependent transformation thermotics (Part I), our experimental demonstration of the macroscopic thermal diode (Part II), and the temperature dependence of $\kappa_1$ and $\kappa_2$ (Part III).
[32] T. Han, T. Yuan, B. Li, and C. Qiu, Sci. Rep. **3**, 1593 (2013).
[33] P. Y. Chen and A. Alù, ACS Nano **5**, 5855 (2011).
[34] W. Zhang, W. M. Zhu, H. Cai, M. J. Tsai, G. Lo, D. P. Tsai, H. Tanoto, J. Teng, X. Zhang, D. Kwong, and A. Liu, IEEE J. Sel. Top. Quantum Electron. **19**, 4700306 (2013).
[35] R. F. Wang, Z. L. Mei, X. Y. Yang, X. Ma, and T. J. Cui, Phys. Rev. B **89**, 165108 (2014).
[36] J. P. Huang and K. W. Yu, Phys. Rep. **431**, 87 (2006).
[37] D. Oh, C. Ko, S. Ramanathan, and D. G. Cahill, Appl. Phys. Lett. **96**, 151906 (2010).
[38] R. Zheng, J. Gao, J. Wang, and G. Chen, Nat. Commun. **2**, 289 (2011).
[39] K. S. Siegert, F. R. L. Lange, E. R. Sittner, H. Volker, C. Schlockermann, T. Siegrist, and M. Wuttig, Rep. Prog. Phys. **78**, 013001 (2015).
[40] T. Omori and R. Kainuma, Nature (London) **502**, 42 (2013).
[41] T. C. Han, X. Bai, J. T. L. Thong, B. W. Li, and C. W. Qiu, Adv. Mater. **26**, 1731 (2014).
[42] N. Q. Zhu, X. Y. Shen, and J. P. Huang, AIP Adv. **5**, 053401 (2015).